

Shortcuts for Electron-Transfer through the Secondary Structure of Helical Oligo-1,2-naphthylenes

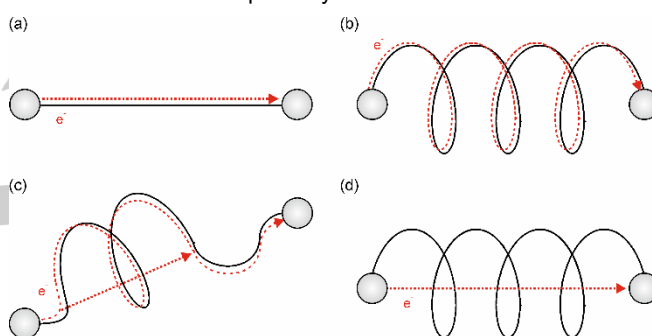
Alessandro Castrogiovanni,[†] Patrick Herr,[†] Christopher B. Larsen, Xingwei Guo,[‡] Christof Sparr,^{*} and Oliver S. Wenger^{*}

Abstract: Atropisomeric 1,2-naphthylene scaffolds provide access to donor-acceptor compounds with helical oligomer-based bridges, and transient absorption studies reveal a highly unusual dependence of the electron transfer rate on oligomer length, which is due to their well-defined secondary structure. Close non-covalent intramolecular contacts enable shortcuts for electron transfer that would otherwise have to occur over longer distances along covalent pathways, reminiscent of the behavior seen for certain proteins. The simplistic picture of tube-like electron transfer can describe this superposition of different pathways including both the covalent helical backbone as well as non-covalent contacts, contrasting the wire-like behavior reported many times before for more conventional molecular bridges. The exquisite control over the molecular architecture, achievable with the configurationally stable and topologically defined 1,2-naphthylene-based scaffolds, is of key importance for the tube-like electron transfer behavior. Our insights are relevant for the emerging field of multi-dimensional electron transfer and for possible future applications in molecular electronics.

1. Introduction

Photoinduced electron transfer (PET) in artificial systems typically relies on linear, rigid rod-like compounds in which the conformational degrees of freedom are restricted, leading to relatively well-defined molecular geometries and donor-acceptor separations (Scheme 1a). Such design simplifies investigations of the influence of driving-force,^[1] donor-acceptor distance,^[2] or bridge structure^[3] on electron transfer rates (k_{ET}). Oligo-*p*-phenylenes are a prototypical class of molecular wires,^[4] but recently oligo-*o*-phenylenes emerged as isomeric alternatives with intriguing properties because of their possible folding into helical secondary structures.^[5] In such helical foldamers, multiple electron transfer pathways begin to compete with one another. On the one hand, electron transfer can still occur along the covalent backbone of the wire (Scheme 1b) like in the linear oligo-*p*-phenylenes, but on the other hand there can now be pathways

involving non-covalent contacts between structural elements that are close in three-dimensional space but not directly connected to one another (Scheme 1d). As long as such conformationally dynamic systems are considered, it remains extremely difficult to distinguish between different pathways (Scheme 1c) because different interconverting conformers can be present on the timescale of the electron transfer event. For this reason, a prior study of dynamic oligo-*o*-phenylene bridged donor-acceptor compounds provided entangled results with limited insight into the actual electron transfer pathways.^[6]



Scheme 1. (a) Electron transfer (ET) through linear wires; (b) ET across the covalent backbone of a helical structure; (c) conformational flexibility complicates the assessment of the relative importance of covalent versus non-covalently pathways; (d) ET pathway involving non-covalent contacts in a helical structure.

Recently, some of us discovered a stereoselective aldol condensation leading to configurationally stable, atropisomeric oligo-1,2-naphthylenes which do not suffer from the problem of rapid interconversion between different wire conformers on the electron transfer timescale, because they are composed of biaryls with defined configuration of stereogenic axes.^[7]

As the understanding of one-dimensional electron transfer (Scheme 1a) gets increasingly complete, there is now growing interest in multi-dimensional electron transfer (Scheme 1b-d), for example in foldamers,^[8] π -stacked,^[9] forked^[10] or circular structures.^[11] The motivations for such research are diverse and include for example the ambition to construct light-harvesting and charge-separating systems that emulate natural photosynthesis, to enhance the efficiency of organic light emitting diodes (OLEDs), or the desire to control electron transfer pathways in future molecular electronics applications. Donor-bridge-acceptor compounds with well-defined molecular structures are ideally suited to explore the fundamentals of multi-dimensional electron transfer, and in our oligo-1,2-naphthylenes the type of unfolding illustrated in Scheme 1c is impossible. Consequently, we are able to get unusually direct insight into the combination of the

[*] A. Castrogiovanni, P. Herr, Dr. C. B. Larsen, Dr. X. Guo, Prof. Dr. C. Sparr, Prof. Dr. O. S. Wenger
Department of Chemistry, University of Basel
St. Johannis-Ring 19, 4056 Basel (Switzerland)
E-mail: christof.sparr@unibas.ch, oliver.wenger@unibas.ch

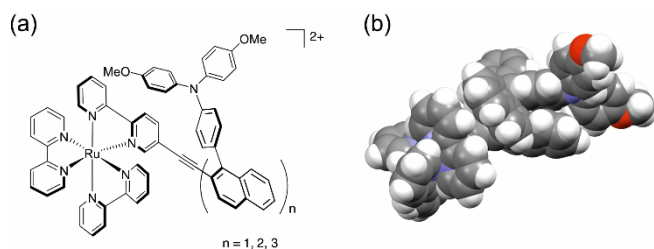
[†] These two authors contributed equally.

[‡] Current address: Center of Basic Molecular Science (CBMS), Department of Chemistry, Tsinghua University, Beijing 100084 (China).

Supporting information for this article is given via a link at the end of the document.

COMMUNICATION

pathways illustrated in Scheme 1b/d, which are of significant interest for the abovementioned applications in solar energy conversion, lighting, and molecular electronics.



Scheme 2. (a) Donor-acceptor dyads synthesized and investigated in this work. (b) Space-filling model of the dyad with $n = 3$ (compound **W3**).

Quantitative information on electron transfer pathways is often extractable from distance dependence studies of electron transfer rates,^[12] and therefore we synthesized three donor-acceptor dyads (Scheme 2a) comprised of variable-length 1,2-naphthylene bridges ($n = 1, 2, 3$). The choice of triarylamine (TAA) and $[\text{Ru}(\text{bpy})_3]^{2+}$ as electron donor and electron acceptor units was mainly motivated by their favorable electrochemical and optical spectroscopic properties, providing unambiguous observables in time-resolved laser spectroscopy.^[6, 13] A space-filling molecular model of the dyad with $n = 3$ (Scheme 2b) illustrates the steric congestion caused by the 1,2-naphthylene based wire backbone, and it becomes evident that pathways involving non-covalent contacts can potentially contribute to electron transfer between TAA and $[\text{Ru}(\text{bpy})_3]^{2+}$ in such structures. To some extent, the situation in our dyads resembles that encountered in proteins, where electron transfer along the covalent primary structure is often preferable, but where individual steps involving non-covalent contacts across the tertiary structure can make important contributions.^[14] In artificial systems, such events are yet hardly explored for the reasons outlined above (Scheme 1).

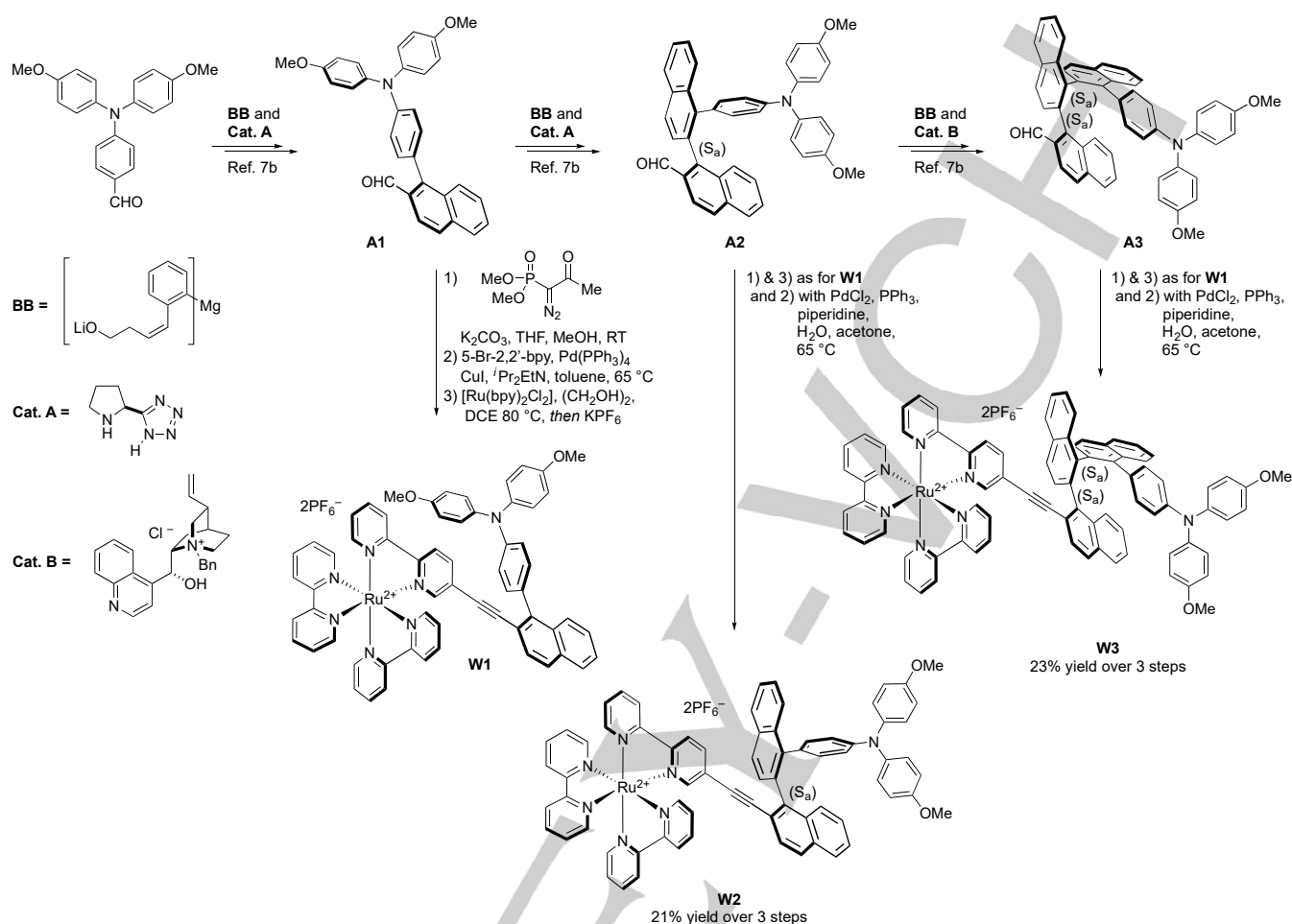
2. Synthesis

Using an iterative oligo-1,2-naphthylene synthesis by the addition of a building block **BB** followed by a catalyst-induced formation of a naphthaldehyde,^[6] precursor **A1** was readily accessible (Scheme 2). The shortest dyad **W1** ($n = 1$) was in turn prepared by conversion of the aldehyde of **A1** to a terminal alkyne by using the Ohira-Bestmann reagent, allowing the subsequent installation of the bipyridine moiety through a Sonogashira cross-coupling. The free ligand was complexed with $[\text{Ru}(\text{bpy})_2\text{Cl}_2]$, delivering the molecular dyad **W1** ($n = 1$) with a covalent distance between the triarylamine (TAA) *N*-atom and the Ru(II) center of 17.5 Å and notably, a drastically shorter spatial separation (7.0 Å). In order to

study the impact of covalent and through-space separation on the PET properties, we next synthesized a homologous system with a longer donor-acceptor distance. We thus converted aldehyde **A2** to the corresponding alkyne under the conditions employed for the synthesis of **W1**, but found that the following Sonogashira cross-coupling was ineffective, presumably due to competitive oxidative pathways. However, this complication could be obviated by performing the cross-coupling under copper-free conditions to access the bipyridine ligand poised for ensuing complexation to provide **W2** ($n = 2$) as a 1 : 1 mixture of (*S_a*)- Δ and (*S_a*)- Λ diastereomers. Compared to **W1**, the homologous dyad **W2** contains a configurationally stable stereogenic axis, resulting in an increased covalent distance of 21.7 Å, which is about twice the length of spatial separation of the donor *N*-atom and Ru (10.3 Å). The possibility of controlling the configuration and the secondary structure of oligo-1,2-naphthylenes to govern the spatial relationship of substituents prompted us to devise a wire with two stereogenic axes. Following the synthetic approach for the preparation of dyad **W2**, the enantio- and diastereoisomerically-defined aldehyde **A3** could be converted to the corresponding dyad **W3** with three naphthylene repeating units. The (*S_a*,*S_a*) configuration of the stereogenic axes ensures a maximal covalent separation of 26.2 Å, which is approximately 10 Å longer than the through-space distance. The $[\text{Ru}(\text{bpy})_3]^{2+}$ photosensitizer unit in all three dyads is present as a mixture of Δ and Λ stereoisomers.

3. Electron transfer

The $[\text{Ru}(\text{bpy})_3]^{2+}$ photosensitizer of all dyads can be selectively excited at 532 nm (Fig. S1), and transient absorption spectra recorded immediately after the 10-ns laser pulses (Fig. 1a) are essentially a superposition of $[\text{Ru}(\text{bpy})_3]^+$ (Fig. 1b) and TAA^{•+} (Fig. 1c) as is evident from UV-Vis spectroelectrochemical measurements. This observation indicates that electron transfer from TAA to photoexcited $[\text{Ru}(\text{bpy})_3]^{2+}$ occurs on a timescale faster than 10 ns. The redox properties of the TAA donor and the $[\text{Ru}(\text{bpy})_3]^{2+}$ photosensitizer are insensitive to bridge elongation (Fig. S2–S4), and cyclic voltammetry yields potentials around 0.70 V vs SCE for the TAA^{+/0} and -1.15 V vs SCE for the $[\text{Ru}(\text{bpy})_3]^{2+/+}$ redox couples in all three dyads. Given an excited-state energy of 2.03 eV (based on the ³MLCT luminescence of the **W2** dyad in butyronitrile at 77 K, Fig. S5), we therefore estimate that one-electron reduction of the ³MLCT-excited $[\text{Ru}(\text{bpy})_3]^{2+}$ units of our dyads occurs at potentials near 0.88 V vs SCE. Consequently, the reaction free energy (ΔG_{ET}^0) for electron transfer from TAA to ³MLCT-excited $[\text{Ru}(\text{bpy})_3]^{2+}$ is around -0.2 eV for all dyads (Table S1), because TAA is oxidized near 0.7 V and photoexcited $[\text{Ru}(\text{bpy})_3]^{2+}$ is reduced near 0.9 V vs SCE. As noted above, this process occurs within the duration of the excitation laser pulses (Fig. S6), and therefore cannot be temporally resolved by nanosecond laser flash photolysis.



Scheme 3. Synthesis of donor-acceptor dyads **W1-3**.

The transient absorption signals of the observable $[\text{Ru}(\text{bpy})_3]^+$ and TAA^{*+} photoproducts (Fig. 1a) start to decay immediately after the end of the pulses (Fig. 2a-c) as a result of the spontaneously occurring thermal reverse electron transfer from reduced acceptor to oxidized donor. All decays are mono-exponential, and for a given dyad they are exactly alike irrespective of whether $[\text{Ru}(\text{bpy})_3]^+$ (red traces in Fig. 2a) or TAA^{*+} is monitored (blue traces in Fig. 2a), diagnostic of intramolecular reverse electron transfer, in the course of which the reduced acceptor and the oxidized donor disappear with identical kinetics. Based on the potentials for the $\text{TAA}^{*+/0}$ and $[\text{Ru}(\text{bpy})_3]^{2+/+}$ redox couples given above, this thermal reverse reaction is associated with ΔG_{ET}^0 of ca. -1.8 eV. Evidently, the thermal reverse electron transfer from $[\text{Ru}(\text{bpy})_3]^+$ to TAA^{*+} has a far greater driving-force (1.8 eV) than the initial electron transfer from TAA to photoexcited $[\text{Ru}(\text{bpy})_3]^{2+}$ (0.2 eV), yet the thermal reverse process occurs on a much slower timescale (ca. 1 μs , Fig. 2a) than the initial photoinduced reaction (< 10 ns, see above). This is not an uncommon observation in molecular dyads and triads of this type, and it is often attributed to the inverted driving-force regime of Marcus

theory, in which electron transfer rates decrease with increasing driving-force.^[1d, 2a, 15]

Single-exponential fits to the decay data in Fig. 2 yield rate constants (k_{ET}) decreasing from $(8.2 \pm 0.4) \times 10^6 \text{ s}^{-1}$ for **W1** to $(6.3 \pm 0.3) \times 10^6 \text{ s}^{-1}$ for **W2** and finally $(5.2 \pm 0.3) \times 10^6 \text{ s}^{-1}$ for **W3** (Table 1). Thus, k_{ET} depends very weakly on dyad length, exhibiting a decrease by only a factor of 1.6 between **W1** and **W3**. This finding is highly unusual as becomes evident by comparison to previously disclosed distance dependence data obtained from dyads with oligo-*p*-phenylene bridges, where each additional phenylene unit typically causes a decrease of k_{ET} by a factor of 10.^[16] The elongation by two *o*-naphthyl units when going from **W1** to **W3** therefore causes a decrease of k_{ET} that is roughly a factor of 60 lower than the expectable decrease associated with the elongation by two *p*-phenylene units. Thus, our oligo-1,2-naphthylene bridges mediate long-range electron transfer with much faster rates than the prototypical oligo-*p*-phenylene wires. This is a remarkable finding, which could not be anticipated at the outset of this project.

Energy minimized ground-state DFT calculations were used to estimate the donor-acceptor distances in our dyads (Fig. S8; see

COMMUNICATION

SI page S29 for details), leading to values between 17.5 ($n = 1$) and 26.2 Å ($n = 3$) when measuring the distance between the TAA *N*-atom and the Ru(II) center along the shortest covalent pathway through all naphthylene units ($r_{\text{DA, cov}}$). Alternatively, values ranging from 7.0 ($n = 1$) to 15.7 Å ($n = 3$) are obtained when determining the distance between the two respective atoms directly through space ($r_{\text{DA, ts}}$). Semi-logarithmic plots of k_{ET} versus distance are linear (Fig. 2d), in line with the commonly observed exponential distance dependence of k_{ET} in the tunneling regime, where the bridge imposes a barrier through which the electrons tunnel from the donor to the acceptor. The distance decay constant (β) in eq. 1 describes the steepness of the exponential decrease of k_{ET} , and $k_{\text{ET}}^{(0)}$ is the electron transfer rate when the donor and the acceptor are in van der Waals contact distance.^[14d] The physical origin of the exponential function in eq. 1 are exponentially decreasing orbital overlaps as described by superexchange theory.^[17] Regardless of whether the $r_{\text{DA, cov}}$ or the $r_{\text{DA, ts}}$ values from above are used, a β value of 0.05 Å^{-1} is obtained for our dyads (Fig. 2d), which is much lower than the typical β -values of oligo-*p*-phenylenes and closely related bridges ($0.5 - 0.8 \text{ Å}^{-1}$).^[16] In principle, β is not a bridge-specific parameter, but instead depends on the entire combination of donor, bridge, and acceptor,^[2c, 18] but nevertheless this comparison between β values is meaningful because some of the previously investigated phenylene-bridged systems involved similar $[\text{Ru}(\text{bpy})_3]^{2+}$ and tertiary amine donors as in dyads **W1-W3**.^[19] Given β values that are lower by a factor of 10-16 in oligo-1,2-naphthylenes than in oligo-*p*-phenylenes, one can argue that our new wires perform by at least an order of magnitude better.

$$k_{\text{ET}}(d) = k_{\text{ET}}^{(0)} \cdot \exp[-\beta \cdot d] \quad (\text{eq. 1})$$

With a β value as low as 0.05 Å^{-1} , a hopping rather than tunneling mechanism could in principle be operative.^[12, 20] In the electron hopping process, individual bridge units are temporarily reduced before the transferring electron reaches the thermodynamic sink at the acceptor. Alternatively, in the hole hopping picture, the bridge units are transiently oxidized before the hole reaches the donor. The electron reduction potential of naphthalene is -2.49 V vs SCE^[21] and the $[\text{Ru}(\text{bpy})_3]^{2+/+}$ potential is -1.15 V vs SCE (see above), hence the temporary reduction of a naphthalene unit by $[\text{Ru}(\text{bpy})_3]^+$ is endergonic by ca. 1.3 eV . The one-electron oxidation of naphthalene requires a potential of 1.54 V vs SCE,^[21] whereas the $\text{TAA}^{+/0}$ potential is 0.70 V vs SCE, and consequently the hole transfer from $\text{TAA}^{+/0}$ to naphthalene is endergonic by ca. 0.8 eV . On this basis, both electron and hole hopping processes are unlikely, and we conclude that the unusually shallow distance dependence observable for our oligo-1,2-naphthylenes is likely due to an unusually efficient tunneling process.

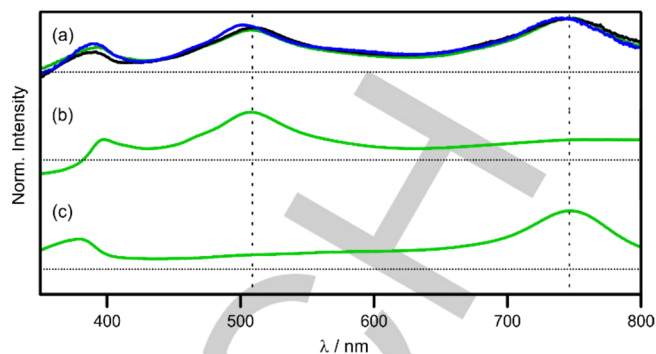


Figure 1. (a) Transient absorption spectra recorded after excitation of $20 \mu\text{M}$ solutions of the dyads from Scheme 1 in acetonitrile (blue, $n = 1$; green, $n = 2$; black, $n = 3$). Excitation occurred at 532 nm with laser pulses of ca. 10 ns duration, spectra were recorded by integration over 200 ns without delay. (b) Spectro-electrochemical UV-Vis difference spectrum recorded from a de-aerated 1 mM solution of the dyad with $n = 2$ in acetonitrile while applying a potential of -1.3 V vs. SCE. (c) Spectro-electrochemical UV-Vis difference spectrum obtained from the same solution while applying a potential of 0.9 V vs. SCE. The UV-Vis spectra prior to applying any potential served as baselines in (b) and (c).

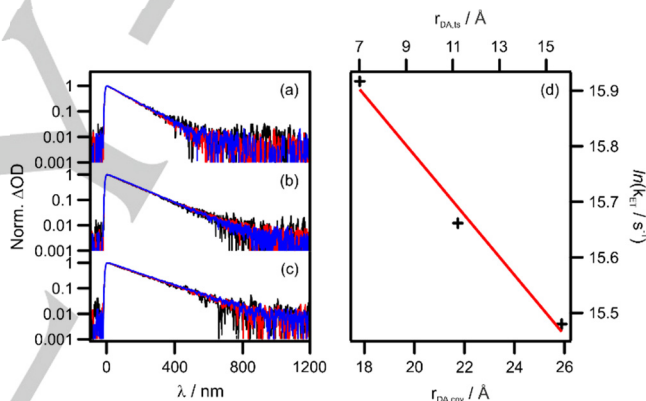


Figure 2. Decay of the transient absorption signals at ca. 390 nm (black), 510 nm (red) and 745 nm (blue) for (a) $n = 1$, (b) $n = 2$ and (c) $n = 3$ in de-aerated acetonitrile after excitation at 532 nm with laser pulses of ca. 10 ns duration ($T = 20^\circ \text{C}$). (d) ET rates (k_{ET}) as a function of donor-acceptor distance measured through the covalent bridge backbone ($r_{\text{DA, cov}}$) and through space ($r_{\text{DA, ts}}$) in energy-minimized ground-state conformers of the three dyads from Scheme 1.

To gain further insight, we performed temperature-dependent transient absorption studies, from which we determined k_{ET} for the thermal reverse electron transfer from $[\text{Ru}(\text{bpy})_3]^+$ to $\text{TAA}^{+/0}$ in all three dyads between 0 and 50°C (Figure S27). Fitting the temperature dependence of k_{ET} to the semiclassical Marcus-Hush equation (eq. 2) is a common procedure to determine the reorganization energy (λ) and the electronic coupling between the donor and the acceptor (H_{DA}).^[3a] We used the reaction free energies (ΔG_{ET}^0) extracted from cyclic voltammetry (Table S1) as input values, and fitted λ and H_{DA} to the kinetic data in Fig. 3 (see SI page S27 for details).

$$k_{\text{ET}} = \frac{\pi}{\hbar^2 \cdot \lambda \cdot k_B \cdot T} \cdot H_{\text{DA}}^2 \cdot \exp \left[-\frac{(\lambda + \Delta G_{\text{ET}}^0)^2}{4 \cdot \lambda \cdot k_B \cdot T} \right] \quad (\text{eq. 2})$$

Table 1. Electron-transfer parameters for the dyads from Scheme 1: Donor-acceptor distances measured through the covalent bridge backbone ($r_{\text{DA,cov}}$) and through-space in low-energy conformers ($r_{\text{DA,ls}}$), rate constants for ET (k_{ET}) at 20 °C, (negative) reaction free energies (ΔG_{ET}^0), activation free energies ($\Delta G_{\text{ET}}^\ddagger$), reorganization energies (λ), and electronic coupling (H_{DA}) between donor and acceptor.

compd	$r_{\text{DA,cov}}$ [Å]	$r_{\text{DA,ls}}$ [Å]	k_{ET} [s^{-1}]	$-\Delta G_{\text{ET}}^0$ [eV]	$\Delta G_{\text{ET}}^\ddagger$ [meV]	λ [eV]	H_{DA} [cm^{-1}]
$n = 1$	17.5	7.0	$(8.2 \pm 0.4) \cdot 10^6$	1.81 ± 0.05	110 ± 10	1.12 ± 0.04	1.5 ± 0.1
$n = 2$	21.7	10.3	$(6.3 \pm 0.3) \cdot 10^6$	1.79 ± 0.05	120 ± 10	1.07 ± 0.04	1.7 ± 0.1
$n = 3$	26.2	15.7	$(5.2 \pm 0.3) \cdot 10^6$	1.82 ± 0.05	140 ± 10	1.06 ± 0.04	2.1 ± 0.1

The obtained λ values for the three dyads are all within experimental error at ca. 1.1 eV (Table 1), in line with numerous previously investigated systems, including many ET enzymes.^[14c] A λ value of 1.1 eV is furthermore compatible with a simple model^[15a] which treats the donor and the acceptor as two charged spheres (with radii of 4 Å) interacting with each other in electrostatic fashion through CH_3CN (with a dielectric constant of 35.7 and a refractive index of 1.3441).^[22] Thus, there is no unusual behavior of λ in our dyads. The striking finding is that H_{DA} is nearly insensitive to bridge elongation and even slightly increases from $1.5 \pm 0.1 \text{ cm}^{-1}$ to $2.1 \pm 0.1 \text{ cm}^{-1}$ between **W1** and **W3** (Table 1). For superexchange tunneling, a decrease of H_{DA} with increasing r_{DA} is usually observed, typically by factors of 1.2 – 3.0 per Å distance elongation depending on whether saturated or π -conjugated bridges are present.^[14c, 14d, 23] Thus, the unusually shallow distance dependence of k_{ET} in our dyads (Fig. 2d) can be attributed to an uncommon behavior of electronic coupling between donor and acceptor, whereas the reorganization energy shows no unusual effects.

Since the peculiar distance dependence of H_{DA} in our dyads cannot be reconciled in the common framework of electron transfer along the covalent backbone of the molecular bridge, we began to consider the possibility of additional tunneling pathways along non-covalent contacts within the helical oligo-1,2-naphthalene structure. Prior work on C-clamp or U-shaped molecules demonstrated that electron transfer through space and through solvent molecules is typically much slower than along covalent pathways.^[24] However, our oligo-1,2-naphthalene structures are very compact (Scheme 2b), with much shorter non-covalent contacts than in previously investigated model systems, and it is conceivable that these short contacts contribute significantly to H_{DA} . As the length of the molecular bridge increases, the number of such non-covalent contacts increases, and this could explain the peculiar distance dependence of H_{DA} uncovered above.

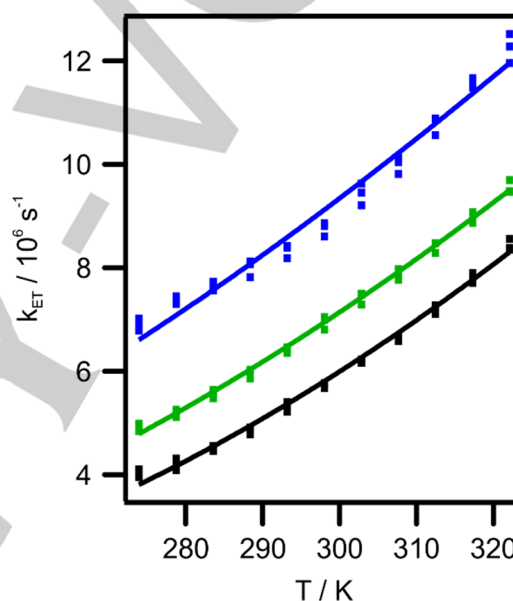


Figure 3. Temperature dependence of k_{ET} for all three dyads recorded at three wavelengths each, fitted to eq. 1.

Ground-state energy-minimized DFT calculations afford qualitative evidence of non-covalent interactions providing possible shortcuts for electron-transfer in our dyads. For instance, there is a short through-space donor-acceptor contact for the **W1** dyad (Fig. 4, top) with a distance of only 7.0 Å between the *N*-atom of TAA and the Ru(II) center, and there are π -interactions between TAA and a naphthylene unit for the **W3** dyad (Fig. 4, bottom). Given that the calculations are on ground-state energy-minimized structures, there are likely many such non-covalent interactions in solution. However, the conformational degrees of freedom of the investigated atropisomeric oligo-1,2-naphthylene dyads **W1-3** are essentially reduced to librational motions between adjacent naphthylene units as well as rotation around the $\text{C}\equiv\text{C}$ triple bond, but unfolding of the helical structures is not possible as discussed above (Scheme 1). Nevertheless, it remains impossible to pinpoint exact transfer paths. The key point here is that the helical oligo-1,2-naphthalene structures impose short non-covalent contacts, and relatively minor thermal fluctuations can readily enable electron transfer across these non-

covalent contacts, complementing the transfer along the covalent backbone.

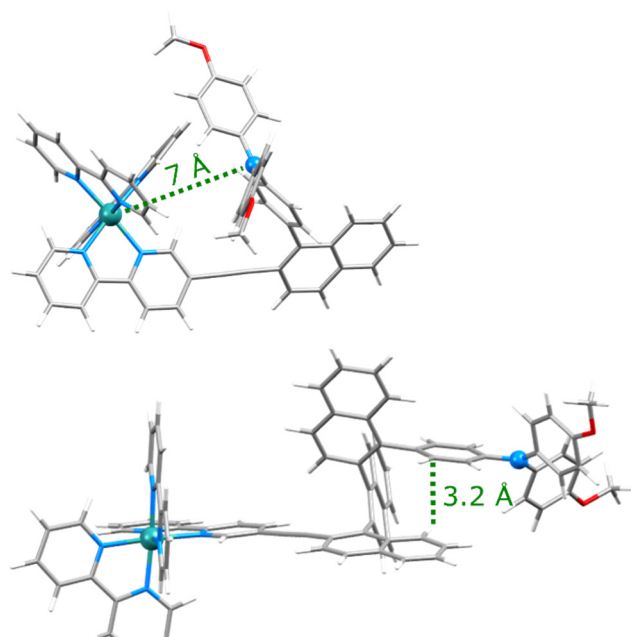


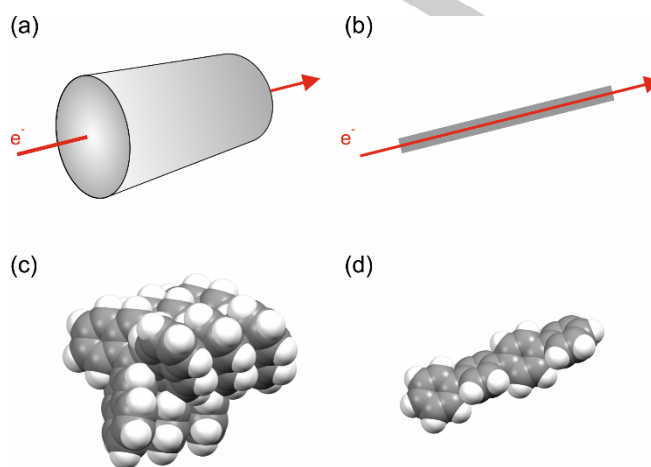
Figure 4. Ground-state geometry-optimized structures of $n = 1$ (top), and $n = 3$ (bottom), obtained from B3LYP/6-31G(d) DFT calculations, highlighting examples of non-covalent short-contacts as possible secondary structure shortcuts for electron-transfer.

4. Summary and conclusions

The electronic coupling (H_{DA}) between the donor and acceptor units in our dyads exhibits a fundamentally different dependence on distance than in the vast majority of previously investigated systems. One-dimensional donor-bridge-acceptor compounds (Scheme 1a) typically exhibit an exponential decrease of H_{DA} in the tunneling regime, whilst electron (or hole) hopping can give rise to more shallow decreases.^[12, 14c, 14d] However, an *increase* of H_{DA} with distance elongation as for the dyads in Scheme 2a (even though weak, from 1.5 ± 0.1 to 2.1 ± 0.1 cm^{-1}) is very rare.^[16b, 25] This suggests that the unusually congested molecular architecture of the oligo-1,2-naphthylene bridges (Scheme 2b) imparts uncommon electronic coupling pathways, likely involving a mixture of covalent and non-covalent contacts present in their three-dimensional structure. Reorganization energies (λ) and reaction free energies (ΔG_{ET}^0) remain essentially constant in all our dyads, supporting the view that the observable weak distance dependence of electron transfer rates (k_{ET}) is indeed caused by unusual electronic coupling effects.

In a somewhat simplistic picture, the atropisomeric and configurationally stable oligo-1,2-naphthylene bridges with their helical structures can be regarded as tube-like objects (Scheme 4a/c), in which the transferring electrons do not strictly follow the circular path of the covalent helical coil, but additionally can also follow shorter paths along the donor-acceptor direction. This is in

contrast to previously investigated linear donor-bridge-acceptor compounds for which the traditional wire-like and strictly one-dimensional picture (Scheme 4b/d) is sufficient.



Scheme 4. (a) Illustration of the tube-like nature of electron transfer in helical oligo-1,2-naphthalene structures; (b) wire-like nature of electron transfer in traditional systems; (c) space-filling model of an oligo-1,2-naphthalene compound comprised of 9 monomer units to illustrate the tube-like nature of the structure; (d) space-filling model of a *p*-phenylene tetramer as a representative wire-like system.

Whilst the oligo-1,2-naphthylene bridges cannot unfold to completely open structures and are forced into the tube-like shape, some conformational fluctuations remain possible, for example librational motions between individual bridge units, or rotation of the photosensitizer around the alkynyl-linker. Thus, it remains impossible to pinpoint exact pathways even in these comparatively rigid structures, but possible shortcuts can readily be identified (Figure 4) without the need for major computational efforts. Similar shortcuts could occur in many other artificial systems where long-range electron transfer takes place, for example in compounds with stacked structures or polymer systems used for organic solar cells.^[26] With conformationally more flexible wires such as for example 1,2-phenylenes, unfolding would readily occur (Scheme 1c), and a far greater ensemble of conformers would be probed on the electron transfer timescale.^[6] Under these conditions, the insights gained above regarding the unusual distance dependence of electronic coupling, shortcuts along non-covalent contacts, and tube-like electron transfer would not be attainable.^[6, 27]

In conclusion, the unique molecular architecture of our new oligo-1,2-naphthylenes leads a combination of electron transfer paths involving both covalent and non-covalent contacts, the superposition of which can be described by the simplistic picture of electron transfer within a tube-like object. This manifests in very weakly distant-dependent electron transfer rates. We are unaware of prior studies that reported similar behavior for other types of artificial molecular bridges.

Current studies are devoted to approaches for increasing 3D topological definition to more clearly disentangle the underlying

contributions of hopping and tunneling pathways to long-range electron transfer.

Acknowledgements

This work was funded by the Swiss NSF through grant numbers 200021_178760 and BSSGI0-155902/1 and the NCCR Molecular

Systems Engineering. We thank Dr. D. Lotter for initial studies and PD Dr. D. Häussinger for NMR support.

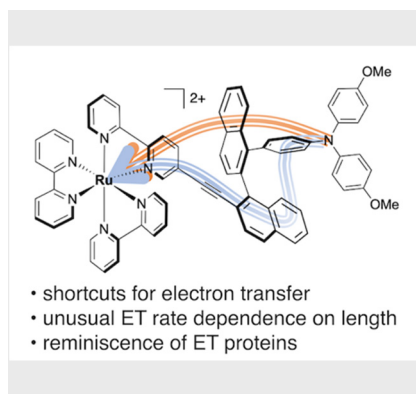
Keywords: electron transfer • donor-acceptor systems • time-resolved spectroscopy • molecular electronics • photochemistry

- [1] a) G. N. Lim, C. O. Obondi, F. D'Souza, *Angew. Chem. Int. Ed.* 2016, 55, 11517-11521; b) L. Favereau, A. Makhal, Y. Pellegrin, E. Blart, J. Petersson, E. Goransson, L. Hammarström, F. Odobel, *J. Am. Chem. Soc.* 2016, 138, 3752-3760; c) M. M. Waskasi, G. Kodis, A. L. Moore, T. A. Moore, D. Gust, D. V. Matyushov, *J. Am. Chem. Soc.* 2016, 138, 9251-9257; d) B. Geiss, C. Lambert, *Chem. Commun.* 2009, 1670-1672; e) M. Wolf, C. Villegas, O. Trukhina, J. L. Delgado, T. Torres, N. Martin, T. Clark, D. M. Guldi, *J. Am. Chem. Soc.* 2017, 139, 17474-17483.
- [2] a) M. Kuss-Petermann, O. S. Wenger, *J. Am. Chem. Soc.* 2016, 138, 1349-1358; b) K. Hu, A. D. Blair, E. J. Piechota, P. A. Schauer, R. N. Sampaio, F. G. L. Parlane, G. J. Meyer, C. P. Berlinguette, *Nat. Chem.* 2016, 8, 853-859; c) B. Albinsson, M. P. Eng, K. Pettersson, M. U. Winters, *Phys. Chem. Chem. Phys.* 2007, 9, 5847-5864; d) K. E. Linton, M. A. Fox, L. O. Palsson, M. R. Bryce, *Chem.-Eur. J.* 2015, 21, 3997-4007; e) P. M. Burrezo, N. T. Lin, K. Nakabayashi, S. Ohkoshi, E. M. Calzado, P. G. Boj, M. A. D. Garcia, C. Franco, C. Rovira, J. Veciana, M. Moos, C. Lambert, J. T. L. Navarrete, H. Tsuji, E. Nakamura, J. Casado, *Angew. Chem. Int. Ed.* 2017, 56, 2898-2902.
- [3] a) J. Sukegawa, C. Schubert, X. Z. Zhu, H. Tsuji, D. M. Guldi, E. Nakamura, *Nat. Chem.* 2014, 6, 899-905; b) R. H. Goldsmith, L. E. Sinks, R. F. Kelley, L. J. Betzen, W. H. Liu, E. A. Weiss, M. A. Ratner, M. R. Wasielewski, *Proc. Natl. Acad. Sci. U. S. A.* 2005, 102, 3540-3545; c) Y. S. Luo, M. Wächter, K. Barthelme, A. Winter, U. S. Schubert, B. Dietzek, *Chem. Commun.* 2019, 55, 5251-5254; d) A. Arrigo, A. Santoro, F. Puntoriero, P. P. Lainé, S. Campagna, *Coord. Chem. Rev.* 2015, 304, 109-116; e) M. Krzeszewski, E. M. Espinoza, C. Cervinka, J. B. Derr, J. A. Clark, D. Borchardt, G. J. O. Beran, D. T. Gryko, V. I. Vullev, *Angew. Chem. Int. Ed.* 2018, 57, 12365-12369.
- [4] a) B. Schlicke, P. Belser, L. De Cola, E. Sabbioni, V. Balzani, *J. Am. Chem. Soc.* 1999, 121, 4207-4214; b) A. C. Benniston, A. Harriman, *Chem. Soc. Rev.* 2006, 35, 169-179.
- [5] a) E. Ohta, H. Sato, S. Ando, A. Kosaka, T. Fukushima, D. Hashizume, M. Yamasaki, K. Hasegawa, A. Muraoka, H. Ushiyama, K. Yamashita, T. Aida, *Nat. Chem.* 2011, 3, 68-73; b) C. S. Hartley, *Acc. Chem. Res.* 2016, 49, 646-654; c) M. Rickhaus, M. Mayor, M. Juricek, *Chem. Soc. Rev.* 2016, 45, 1542-1556.
- [6] S. Malzkuhn, X. Guo, D. Häussinger, O. S. Wenger, *J. Phys. Chem. A* 2019, 123, 96-102.
- [7] a) D. Lotter, M. Neuburger, M. Rickhaus, D. Häussinger, C. Sparr, *Angew. Chem. Int. Ed.* 2016, 55, 2930-2933; b) A. Link, C. Sparr, *Chem. Soc. Rev.* 2018, 47, 3804-3815.
- [8] a) A. Méndez-Ardoy, N. Markandeya, X. S. Li, Y. T. Tsai, G. Pecastaings, T. Buffeteau, V. Maurizot, L. Muccioli, F. Castet, I. Huc, D. M. Bassani, *Chem. Sci.* 2017, 8, 7251-7257; b) X. S. Li, N. Markandeya, G. Jonusauskas, N. D. McClenaghan, V. Maurizot, S. A. Denisov, I. Huc, *J. Am. Chem. Soc.* 2016, 138, 13568-13578; c) M. Wolfs, N. Delsuc, D. Veldman, N. Van Anh, R. M. Williams, S. C. J. Meskers, R. A. J. Janssen, I. Huc, A. P. H. J. Schenning, *J. Am. Chem. Soc.* 2009, 131, 4819-4829.
- [9] a) A. R. Mallia, P. S. Salini, M. Hariharan, *J. Am. Chem. Soc.* 2015, 137, 15604-15607; b) Y. L. Wu, N. S. Bobbitt, J. L. Logsdon, N. E. Powers-Riggs, J. N. Nelson, X. L. Liu, T. C. Wang, R. Q. Snurr, J. T. Hupp, O. K. Farha, M. C. Hersam, M. R. Wasielewski, *Angew. Chem. Int. Ed.* 2018, 57, 3985-3989; c) S. Bhosale, A. L. Sisson, P. Talukdar, A. Furstenberg, N. Banerji, E. Vauthey, G. Bollot, J. Mareda, C. Roger, F. Wurthner, N. Sakai, S. Matile, *Science* 2006, 313, 84-86.
- [10] M. Delor, S. A. Archer, T. Keane, A. Meijer, I. V. Sazanovich, G. M. Greetham, M. Towrie, J. A. Weinstein, *Nat. Chem.* 2017, 9, 1099-1104.
- [11] C. B. Larsen, O. S. Wenger, *Angew. Chem. Int. Ed.* 2018, 57, 841-845.
- [12] M. Cordes, B. Giese, *Chem. Soc. Rev.* 2009, 38, 892-901.
- [13] H. C. Schmidt, C. B. Larsen, O. S. Wenger, *Angew. Chem. Int. Ed.* 2018, 57, 6696-6700.
- [14] a) T. R. Prytkova, V. V. Shunaev, O. E. Glukhova, I. V. Kurnikov, *J. Phys. Chem. B* 2015, 119, 1288-1294; b) J. J. Regan, S. M. Risser, D. N. Beratan, J. N. Onuchic, *J. Phys. Chem. B* 1993, 97, 13083-13088; c) J. R. Winkler, H. B. Gray, *J. Am. Chem. Soc.* 2014, 136, 2930-2939; d) H. B. Gray, J. R. Winkler, *Proc. Natl. Acad. Sci. U. S. A.* 2005, 102, 3534-3539.
- [15] a) R. A. Marcus, N. Sutin, *Biochim. Biophys. Acta* 1985, 811, 265-322; b) P. Y. Chen, T. D. Westmoreland, E. Danielson, K. S. Schanze, D. Anthon, P. E. Neveux, T. J. Meyer, *Inorg. Chem.* 1987, 26, 1116-1126.
- [16] a) E. A. Weiss, M. J. Ahrens, L. E. Sinks, M. A. Ratner, M. R. Wasielewski, *J. Am. Chem. Soc.* 2004, 126, 9510-9511; b) O. S. Wenger, *Chem. Soc. Rev.* 2011, 40, 3538-3550; c) J. J. Shen, Y. W. Zhong, *Sci Rep* 2015, 5, doi: 10.1038/srep13835; d) S. Welter, N. Salluce, P. Belser, M. Groeneveld, L. De Cola, *Coord. Chem. Rev.* 2005, 249, 1360-1371; e) M. T. Indelli, C. Chiorboli, L. Flamigni, L. De Cola, F. Scandola, *Inorg. Chem.* 2007, 46, 5630-5641.
- [17] a) H. M. McConnell, *J. Chem. Phys.* 1961, 35, 508-515; b) M. Natali, S. Campagna, F. Scandola, *Chem. Soc. Rev.* 2014, 43, 4005-4018.
- [18] a) F. D. Lewis, J. Q. Liu, W. Weigel, W. Rettig, I. V. Kurnikov, D. N. Beratan, *Proc. Natl. Acad. Sci. U. S. A.* 2002, 99, 12536-12541; b) O. S. Wenger, *Acc. Chem. Res.* 2011, 44, 25-35.
- [19] a) D. Hanss, O. S. Wenger, *Inorg. Chem.* 2008, 47, 9081-9084; b) D. Hanss, O. S. Wenger, *Inorg. Chem.* 2009, 48, 671-680.
- [20] a) S. Welter, F. Lafolet, E. Cecchetto, F. Vergeer, L. De Cola, *ChemPhysChem* 2005, 6, 2417-2427; b) E. A. Weiss, M. J. Tauber, R. F. Kelley, M. J. Ahrens, M. A. Ratner, M. R. Wasielewski, *J. Am. Chem. Soc.* 2005, 127, 11842-11850; c) W. B. Davis, W. A. Svec, M. A. Ratner, M. R. Wasielewski, *Nature* 1998, 396, 60-63.
- [21] M. Montalti, A. Credi, L. Prodi, M. T. Gandon, *Handbook of photochemistry*, 3rd edition, CRC/Taylor & Francis, Boca Raton, 2006.
- [22] M. Kuss-Petermann, O. S. Wenger, *Phys. Chem. Chem. Phys.* 2016, 18, 18657-18664.
- [23] P. J. Low, *Coord. Chem. Rev.* 2013, 257, 1507-1532.
- [24] a) K. Kumar, Z. Lin, D. H. Waldeck, M. B. Zimmt, *J. Am. Chem. Soc.* 1996, 118, 243-244; b) J. M. Nadeau, M. Liu, D. H. Waldeck, M. B. Zimmt, *J. Am. Chem. Soc.* 2003, 125, 15964-15973; c) B. M. Graff, D. N. Lamont, M. F. L. Parker, B. P. Bloom, C. E. Schafmeister, D. H. Waldeck, *J. Phys. Chem. A* 2016, 120, 6004-6013.
- [25] a) C. Stangel, C. Schubert, S. Kuhri, G. Rotas, J. T. Margraf, E. Regulska, T. Clark, T. Torres, N. Tagmatarchis, A. G. Coutsolelos, D. M. Guldi, *Nanoscale* 2015, 7, 2597-2608; b) E. A. Weiss, M. J. Ahrens, L. E. Sinks, A. V. Gusev, M. A. Ratner, M. R. Wasielewski, *J. Am. Chem. Soc.* 2004, 126, 5577-5584.
- [26] a) G. Li, R. Zhu, Y. Yang, *Nat. Photonics* 2012, 6, 153-161; b) A. Mishra, P. Bäuerle, *Angew. Chem. Int. Ed.* 2012, 51, 2020-2067; c) F. C. Grozema, L. D. A. Siebbeles, *Int. Rev. Phys. Chem.* 2008, 27, 87-138.
- [27] E. H. Yonemoto, G. B. Saupe, R. H. Schmehl, S. M. Hubig, R. L. Riley, B. L. Iverson, T. E. Mallouk, *J. Am. Chem. Soc.* 1994, 116, 4786-4795.

Entry for the Table of Contents

COMMUNICATION

Taking shortcuts: Phototriggered electron transfer between a triarylamine unit and a ruthenium complex follows shortcuts in the secondary structure of a naphthylene-based molecular bridge, leading to a particularly low distance dependence of reaction rates and overall faster electron transfer.



Alessandro Castrogiovanni,[†] Patrick Herr,[†] Christopher B. Larsen, Xingwei Guo, Christof Sparr,^{*} and Oliver S. Wenger^{*}

Page No. – Page No.

Shortcuts for Electron-Transfer through the Secondary Structure of Helical Oligo-1,2-naphthylenes